Chapter 1

Introduction to Optical Tweezers: Background, System Designs, and Commercial Solutions

Joost van Mameren, Gijs J.L. Wuite, and Iddo Heller

Abstract

Optical tweezers are a means to manipulate objects with light. With the technique, microscopically small objects can be held and steered while forces on the trapped objects can be accurately measured and exerted. Optical tweezers can typically obtain a nanometer spatial resolution, a piconewton force resolution, and a millisecond time resolution, which make them excellently suited to study biological processes from the single-cell down to the single-molecule level. In this chapter, we provide an introduction on the use of optical tweezers in single-molecule approaches. We introduce the basic principles and methodology involved in optical trapping, force calibration, and force measurements. Next, we describe the components of an optical tweezers setup and their experimental relevance in single-molecule approaches. Finally, we provide a concise overview of commercial optical tweezers systems. Commercial systems are becoming increasingly available and provide access to single-molecule optical tweezers experiments without the need for a thorough background in physics.

Key words: Optical tweezers, Optical trap, Radiation pressure, Single molecule, Trap stiffness calibration, Force spectroscopy, Instrument design, Commercial optical tweezers, Molecular motors, DNA–protein interactions

1. Introduction

1.1. History of Optical Tweezers

At the heart of optical tweezers techniques is the interaction between light and matter. The minute forces that are generated in this interaction can be used to displace and trap microscopic objects. In 1970, Ashkin laid the foundations for present-day optical tweezers techniques. At Bell labs, Ashkin observed that micron-sized latex spheres (beads) were attracted toward the center of an argon laser beam of a few mW power (1). It is this attractive force that makes optical trapping possible. Ashkin also observed, however, that the laser light scattered and propelled the beads forward. By using two counterpropagating beams, he managed to avoid forward propulsion, and thus created the first stable

Erwin J.G. Peterman and Gijs J.L. Wuite (eds.), *Single Molecule Analysis: Methods and Protocols*,
Methods in Molecular Biology, vol. 783, DOI 10.1007/978-1-61779-282-3_1, © Springer Science+Business Media, LLC 2011

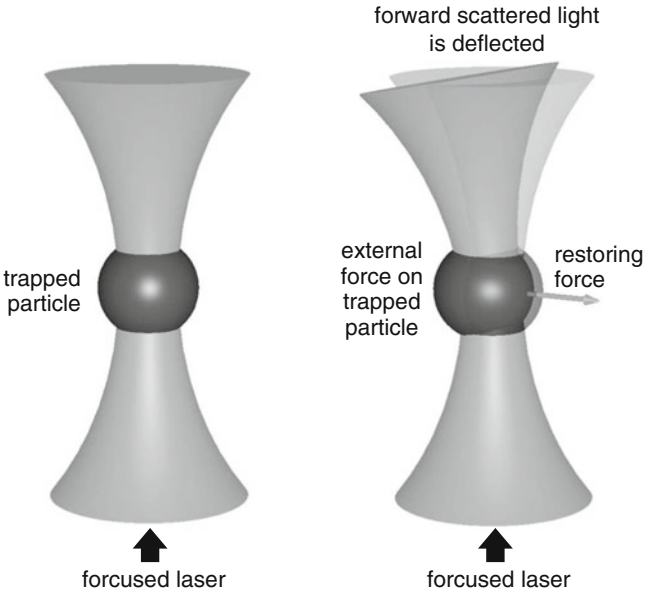

Fig. 1. Schematic of optical trapping. *Left*: A tightly focused laser beam (*cone*) attracts refractive objects (*dark sphere*), such as glass beads, nanoparticles, or even whole cells to its focus. *Right*: External forces pushing or pulling on the particle slightly displace it from the center of the focus, leading to a slight deflection of the forward-scattered laser light. This deflection forms the basis for quantitatively detecting the forces and displacements experienced by the trapped object.

optical trap for beads suspended in water. It was not until 1986 that Ashkin together with Chu and others demonstrated the present form of *optical tweezers* that uses a single, *tightly focused* laser beam to stably trap particles – of diameters between 25 nm and 10 μm – in three dimensions (see Fig. 1, left) (2). Later on, Chu and others used techniques inspired by optical tweezers to trap and cool atoms, which brought him the 1997 Nobel Prize in physics (3, 4).

1.2. Optical Tweezers in Biology

Currently, optical tweezers have found widespread applications in biology (5–7). One of the important reasons for the success of optical tweezers in biology is that it provides biological scientists with "microscopic hands" to manipulate biological objects and feel or exert forces, yet with the same low level of invasiveness as light microscopy techniques. Furthermore, the length scales, time scales, and force scales accessible to optical tweezers are biologically relevant from the single-cell down to the single-molecule level. In 1987, Ashkin presented the first applications of optical tweezers in biology by manipulating individual viruses and living bacteria (8). By a correct choice of laser power and wavelength, photodamage to biological samples could be minimized, which allowed trapping and manipulation of single living cells (9). Since

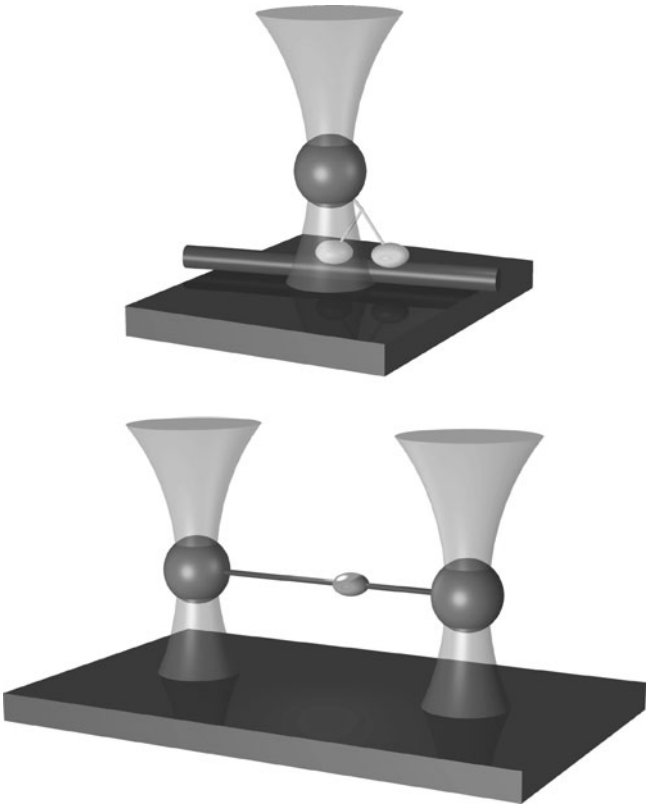

Fig. 2. Prototypical single-molecule optical tweezers assays. *Top*: A single kinesin motor protein bound with its two heads to an optically trapped bead moves along a surface-immobilized microtubule track. Its 8-nm steps, the forces exerted, and the mechanics of the stepping have been elucidated in such assays. *Bottom*: DNA suspended between two optically trapped beads.

the late 1980s, optical tweezers approaches have been extended down to the single-biomolecule level (10–20). In these single-molecule studies, the biomolecules of interest are not themselves trapped directly, but are manipulated through optically trapped microbeads that act as handles and force transducers. A large fraction of this single-molecule work includes the study of the activity of individual motor proteins (10, 14, 20). With optical tweezers, the motion and forces generated by these motor proteins have been studied and controlled to reveal their dynamics and energetics (Fig. 2, top). Another important area of research includes the study of biopolymers, such as DNA (7, 13, 16, 21). In these experiments, the DNA molecule is attached to one or more optically trapped beads which allows stretching the molecule and studying its mechanical properties through force spectroscopy (Fig. 2, bottom). In addition, this layout has been used to study-DNA–protein interactions (12, 15, 19, 22). A wide range of DNA–protein interactions affect the structure of DNA, and thus

the (force-dependent) length of the DNA molecules. In optical tweezers, these length changes can be observed by measuring the displacements of the microbeads. Examples include the study of DNA-binding proteins and the activity of DNA and RNA polymerases.

With the advent of commercial optical tweezers systems in recent years, this powerful single-molecule technique is approaching maturation and is becoming more and more accessible to a wide range of biological scientists. As with the development of commercial fluorescence and AFM techniques, it is to be expected that commercial optical tweezers greatly contribute to our knowledge of biology on the single-molecule level. As a final motivation to read more about optical tweezers: in an interview with Physics Today, Nobel Prize winner Steven Chu said that he would not be surprised if in the coming decennium another Nobel Prize would be attributed to groundbreaking discoveries in molecular biology facilitated by optical tweezers or other single-molecule techniques (23).

2. Principles of Optical Tweezers Techniques

The basic physical principle underlying optical tweezers is the radiation pressure exerted by light when colliding with matter. For macroscopic objects, the radiation pressure exerted by common light sources is orders of magnitude too small to have any measurable effect: we do not feel the light power of the sun pushing us away. However, for objects of microscopic dimensions ($<$100 μm), the radiation pressure of high-intensity light sources is sufficient to facilitate optical trapping.

2.1. Forces in an Optical Trap

When photons enter an object that has a different refractive index than its surrounding medium, part of the momentum of the photons can be transferred to this object. This transfer of momentum is the physical principle that underlies optical trapping (see Fig. 1, right). The forces exerted by photons on an optically trapped object can be divided into two components: the scattering force that pushes the object away from the light source and the gradient force that pulls the object toward the region of highest light intensity. The correct physical description of optical trapping depends on the size d of the trapped object in comparison to the wavelength λ of the trapping light. In the regime $d >> \lambda$, one speaks of the "ray-optics" regime while the regime where $d << \lambda$ is called the Rayleigh regime. In biological experiments where micrometer-sized objects are trapped, the correct description is often in between these two regimes such that neither description

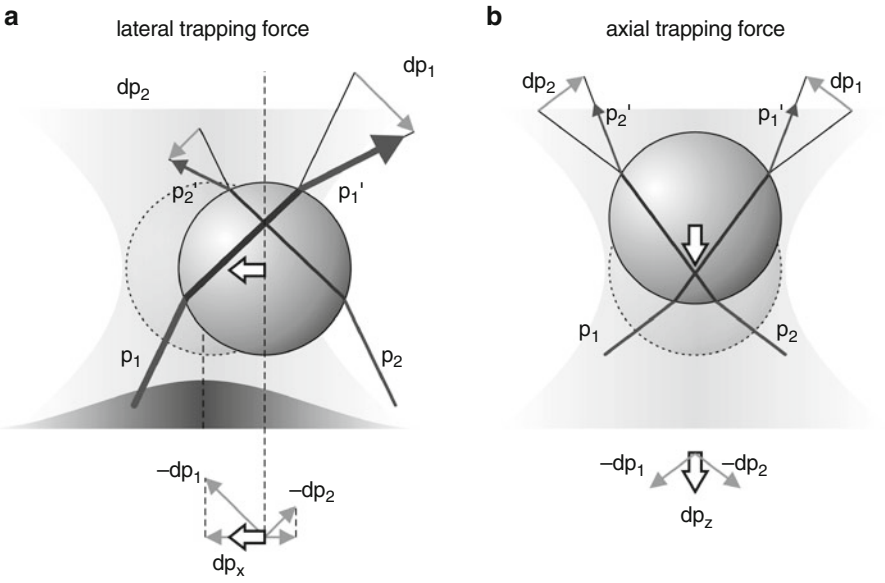

Fig. 3. Forces on an optically trapped particle in the ray-optics regime. (**a**) Lateral gradient force of a Gaussian laser beam profile. (**b**) Axial gradient force toward the focus of the trapping light. The *white arrows* indicate the net restoring force. Note that the scattering component due to reflection by the particle is not indicated.

is quantitatively accurate. To provide a qualitative understanding of optical trapping, we here describe the forces in the more intuitively interpretable ray-optics regime. In the ray-optics regime, the trapping force can be understood in terms of refraction of light rays between media with different indices of refraction (24). Figure 3 qualitatively depicts the origin of the trapping forces in this regime. The lateral gradient restoring force (Fig. 3a) can be understood as follows. If rays p_1 and p_2 have different intensity, the momentum changes of these rays (Δp_1 and Δp_2, respectively) differ in magnitude, causing a net reaction force on the refracting medium in the direction of highest intensity. The x-projection of this force, Δp_x, tends to counteract a displacement from the laser beam axis, pulling the particle toward the center of the beam. The axial gradient force is similarly caused by momentum transfer upon refraction, resulting in a restoring force toward the focus, as in Fig. 3b. The scattering force (not depicted) would cause the object to be propelled out of the focus, along the positive z-direction. The object is stably trapped only if the scattering force along the positive z-direction is compensated by the gradient force along the negative z-direction. To achieve this, a significant fraction of the incident light should come in at large angles, calling for a tightly focused trapping light source typically obtained by using a microscope objective.

2.2. Trap Stiffness

An optical trap forms a three-dimensional potential well for the trapped particle. The particle experiences an attractive force

toward the potential minimum, which is located at a stable position where the trapped particle experiences no net force. Close to the potential minimum, the trap can be approximated to be harmonic, e.g., the attractive force F is directly proportional to the displacement x of the particle according to Hooke's law: $F = -\kappa x$. Here, the spring constant κ has units [N/m] like a mechanical spring and represents the stiffness of the optical trap. Knowledge of the trap stiffness allows accurate quantification of the external forces acting on a trapped particle from a measurement of the particle's displacement. The trap stiffness, however, is a complex function of the intensity profile and wavelength of the laser, the shape and size of the particle, the indices of refraction, and other parameters and is difficult to calculate from first principles. Therefore, the trap stiffness is commonly determined by performing calibration experiments. Using a laser of 1 W, the typical trap stiffness that can be obtained in a single-beam optical trap is in the order of 100 pN/μm.

2.3. Principles of Trap Calibration

To allow quantitative measurement of the forces on optically trapped particles, several calibration methods to measure the trap stiffness have been developed.

Drag force calibration: The simplest way to calibrate an optical trap is to apply an external force of known magnitude and measure the displacement of the trapped particle. The external force is typically generated by inducing a fluid flow. The drag force by a fluid (viscosity η, flow velocity v) on a spherical bead of diameter d is given by Stokes' law: $F = \gamma v$, where γ is the drag coefficient $\gamma = 3\pi\eta d$. The fluid drag displaces the bead from the center of the trap until the drag force is opposite and equal to the restoring force from the optical trap, which yields $\kappa = \gamma v / x$. The trap stiffness can, thus, be obtained by measuring the displacement, x, of a bead of known size due to the fluid flow of a liquid with known viscosity and velocity.

Brownian motion calibration: Another, more accurate calibration procedure is based on the Brownian motion of a bead in an optical trap, caused by the continuous and random collisions with solvent molecules. The stiffness of an optical trap can be calibrated by recording the power spectrum of the displacement fluctuations of a trapped bead of known size, as shown in Fig. 4. The power spectrum $S_x(f)$ describes how the power of these displacement fluctuations is distributed in frequency f and is found to have a Lorentzian shape (25, 26):

$$S_x(f) = \frac{k_B T}{\gamma \pi^2 \left(f_c^2 + f^2\right)},$$

where $k_B T$ is the available thermal energy. The power spectrum exhibits a characteristic corner frequency $f_c \equiv \kappa / 2\pi\gamma$, which is

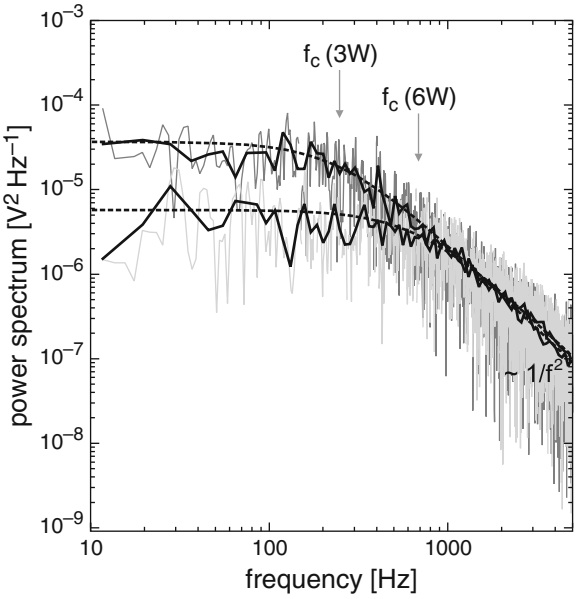

Fig. 4. Power spectra representative of the positional fluctuations of a particle trapped at different laser powers. A 1-μm diameter polystyrene bead is held in an optical trap while the displacement signal in volts is sampled at 195 kHz. The graph shows power spectra of the displacement signal at 3 W (*dark gray*) and at 6 W (*light gray*) laser power. Both the downward shift of the low-frequency plateau S_0 and the upward shift of the corner frequency f_c (see *arrows* at 250 and 650 Hz, obtained from Lorentzian fits) for the stiffer 6 W trap can clearly be observed.

proportional to the trap stiffness. Figure 4 shows that at low frequencies $f << f_c$, the power spectrum is roughly constant, $S_x(f) = S_{x,0} = 4\gamma k_B T/\kappa^2$. At high frequencies $f >> f_c$, however, the power spectrum falls off like $1/f^2$, which is characteristic of free diffusion. The inverse of the corner frequency represents the time response of the optical trap, which is typically in the order of 1–0.1 ms. For shorter timescales, the particle does not "feel" the confinement of the trap which means that behavior of biological systems at timescales more rapid than this response time cannot be detected by the optical tweezers. The two power spectra of Fig. 4, acquired at two different trap stiffnesses, illustrate that when higher trap stiffnesses are used (i.e., by increasing the laser power), the bead fluctuations at low frequencies are reduced and the time response of the optical trap increases. On the other hand, a higher trap stiffness implies smaller bead displacement at a given force which means that more accurate bead displacement detection is required to obtain the same force sensitivity.

It is important to note that, in practice, the detector used to determine the bead position reads *uncalibrated* displacement fluctuations $u(t)$ (i.e., as some voltage rather than as a displacement

in nanometers). The response of the detector R, which has units m/V, relates the displacement to $u(t)$ as $x(t) = Ru(t)$. To fully calibrate an optical trap, the power spectrum of the uncalibrated displacement fluctuations $S_u(f)$ is fitted with a Lorentzian:

$$S_u(f) = \frac{S_{u,0} f_c^2}{(f_c^2 + f^2)}.$$

Once the parameters $S_{u,0}$ and f_c are obtained, the trap stiffness can be calculated using

$$\kappa = \frac{2k_B T}{\pi S_{u,0} f_c} \quad \text{or} \quad \kappa = 2\pi\gamma f_c,$$

and, providing the bead diameter and solvent viscosity are known, the detector response can be calculated using

$$R = \left[\frac{k_B T}{\pi^2 \gamma S_{u,0} f_c^2}\right]^{1/2} \overset{25^\circ C}{=} \left[\frac{5.0 \times 10^{-20} \mathrm{m}^3/\mathrm{s}}{S_{u,0} f_c^2 d}\right]^{1/2}.$$

Finally, to convert uncalibrated displacement data to forces, the displacement signal should be multiplied by R and the trap stiffness such that $F = \kappa x = \kappa R u$.

3. Optical Tweezers Systems

An optical tweezers setup consists of various dedicated components. In this section, we discuss the role of these components in optical tweezers function and performance. Below, we divide and discuss the components in five groups: the trap, the environment of the trap, trap steering, position and force detection, and the environment of the setup. In addition, we also discuss the ability to combine optical tweezers with other techniques and the different optical trapping assays that are typically used in biological experimentation. For illustration, Fig. 5 shows the schematic layout of an optical tweezers setup that combines two steerable optical traps with fluorescence microscopy.

3.1. The Optical Trap

At the heart of every single-beam optical tweezers instrument is the *microscope objective*, which creates a tight focus to form a stable optical trap. Tight focusing implies that a significant fraction of the incident light comes in at large angles such that the scattering force is overcome by the gradient force. The maximum incidence angle of the light Θ_{max} is determined by the numerical aperture (NA) of the objective used to focus the laser beam. This is a measure for the solid angle over which the objective lens can

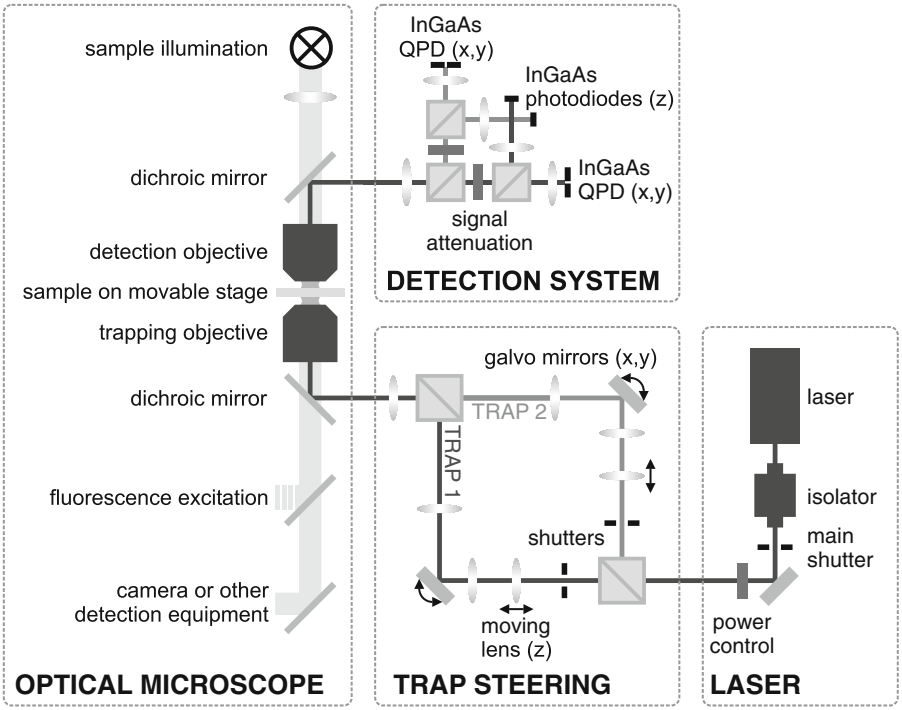

Fig. 5. Optics layout of a typical optical tweezers instrument. The various parts of the system as described in the text are bounded by *dashed boxes*. The depicted layout was adopted from that of the "NanoTracker" commercial optical tweezers platform of JPK Instruments (see Subheading 5).

gather light and is defined as: NA = n sin $\Theta_{\max}$, where n is the refractive index of the immersion medium (i.e., the medium between the objective lens and the sample) and $\Theta_{\max}$ is one-half the angular aperture. The value of n varies between 1.0 for air and ≈1.5 for most immersion oils. For typical oil-immersion objectives, an NA of 1.4 corresponds to a total acceptance angle of the objective of about 130°. To obtain a stable three-dimensional optical trap, the laser beam entering the objective has to be wide enough to fill or overfill the back aperture of the objective. This way, one provides sufficient convergent, high-angle rays that contribute to counteracting the scattering force.

The maximum forces that can be exerted by an optical trap can be enhanced by either increasing the laser power or optimizing the quality of the focal spot of the laser and the refraction of the laser by the trapped particle (i.e., choosing the proper optics and materials with proper optical densities; see below). The laser power can be increased only up to a certain limit, above which more laser light would lead to heating or photodamage of the examined system (often delicate biomaterials) or even of the optics in the instrument (27). Therefore, care must be taken to optimize the quality of the focal spot of the trapping laser. The difference in refractive index of the trapped object n_2 compared to that of the

surrounding medium n_1 determines how strongly the incident rays are refracted and, consequently, how strong the trapping force is. The required balance between gradient and scattering forces yields an optimal refractive index of $n_2 = 1.69$ (5). One often uses silica (glass) particles ($n_2 = 1.37$–1.47) or polystyrene particles ($n_2 = 1.57$). The trapping forces that can be obtained for polystyrene particles are, thus, higher. When using an oil-immersion objective, the refractive index of the immersion oil matches both that of the objective lens and that of the glass of the sample. Therefore, the maximum NA can be achieved with oil-immersion objectives. However, due to the refractive index mismatch between the sample glass and the buffer, spherical aberrations deteriorate the quality of the laser focus when the distance of the focus to the sample surface increases (optical trapping in water with oil-immersion objectives is typically performed within several tens of micrometers of the glass surface) (28). To allow equally stable trapping at any distance to the surface, water-immersion objectives are often used. Despite the fact that the NA is somewhat compromised (typically, NA = 1.2 for water-immersion objectives), the ability to move away from the sample surface without lowering the trap quality can be a good reason to use water-immersion objectives.

For optical trapping, single-mode continuous wave lasers with a Gaussian beam profile (i.e., operated in the lowest, TEM_{00}, mode) are commonly used. The laser power typically ranges from a few hundred milliwatts up to several watts. Important properties of the laser for stable trapping are low intensity fluctuations and high pointing stability (little angular and transverse wandering of the beam). Of particular interest for biological experiments is the wavelength. Since the light intensity at the focus is very high, heating and damage through light absorption by the often delicate biological material need to be considered. Near-infrared lasers (800–1,200 nm, most often the 1,064-nm line from diode-pumped solid-state lasers) are typically used because of the low absorption of biological material as well as water in this spectral range (5).

Although in current biological applications optical traps are most commonly formed by tightly focusing a single laser beam (2), the first stable optical trap was accomplished in 1970 by using two counterpropagating focused laser beams (1). The counterpropagating layout does not require tight focusing such that low NA (<1) objectives or no objective at all may be used. Advantageously, this allows for a larger working distance and lower local light intensity at the trap, making it useful to handle living cells. The "optical stretcher," designed to probe the deformability of individual cells, is a key example of this approach (29).

3.2. Environment of the Trap

Microfluidics: To ascertain well-controlled experimental conditions in single-molecule experiments, it is often useful – if not required – to implement a way to bring the biochemical "ingredients" together under the microscope. The use of microfluidics allows for a fine control over this process by fluid flow of minute volumes of the solutions used. In addition, microfluidic control allows for drag force calibration of the trap, as well as flow stretching of biopolymers, such as DNA (30). An alternative way to induce viscous drag is by moving the fluid reservoir with respect to the trap using a motorized microscope stage. Particularly useful is the combination of either a motorized or a piezoelectric stage with a laminar flow cell. The laminar flow ensures that different buffer flows can be in contact with each other with minimal buffer mixing. By moving the stage to change the position of the trapped beads in the microfluidic device, the buffer conditions can be rapidly exchanged between the regions of different buffer flow. Recently, Brewer et al. extensively reviewed the use of microfluidics devices in single-molecule experiments (31).

Temperature control: In biological experiments, temperature often plays an important role. As in conventional microscopy, temperature-controlled fluidics, stages, and objectives can be used to control the temperature at which biological processes take place. In optical tweezers experiments, temperature control of the objective is, in particular, considered. Objectives with short focal lengths, required to obtain a tight focus, are necessarily in close contact with the trapping region through the immersion medium and act as an effective heat sink. Moreover, apart from the relevance for the temperature of the biological system, temperature control of the objective can be beneficial for the performance of the optical tweezers as well. The high laser intensities in optical trapping may produce heating of the optical components, thus causing optical drift, increased stabilization time, and/or decreased spatial resolution. A millikelvin temperature-stabilized objective has been employed to obtain base pair resolution in optical tweezers experiments on DNA (32). Finally, judicious design and analysis of the experiment are required when large temperature fluctuations are anticipated. Among other issues, the reliability of (real time) calibration of optical tweezers using Brownian fluctuations is impacted by significant temperature fluctuations.

3.3. Position and Force Detection

The key to quantitative optical trapping is the accurate detection of the position of the particle in an optical trap. Within the volume of the laser focus, the displacement of the particle from its equilibrium position is directly proportional to the forces acting on this particle.

Several techniques have been developed for sensitive position detection which are discussed below.

Lateral position and force detection – The simplest position-detection scheme relies on video-based imaging of a bead in the optical trap. Using centroid-tracking or template-matching algorithms, the position of one or multiple beads can be obtained with sub-pixel resolution (down to several nanometers) either by off-line or online digital video analysis (33, 34). Although video-based position detection is simple and direct, it is limited in time resolution by the video acquisition rate (from typically 25 up to 100 Hz with faster cameras). More dedicated imaging techniques, where one bead is directly imaged on a position-sensitive detector (PSD) or quadrant photodiode (QPD), provide a higher time resolution, but require high magnifications and are thus limited in range and signal-to-noise ratio (35, 36). Besides allowing the calculation of the active forces in a biological system when the trap stiffness is known, imaging also provides spatial information on the studied system; observation of the absolute position of beads in the camera's field of view can provide information on the length scale of a biological system, such as a stretched biopolymer between two beads or the motion of a molecular motor through the field of view, independent of the optical trapping (cf. Fig. 2).

The highest time resolution (~μs) and spatial resolution (~pm) are currently obtained with laser-based interferometry techniques for position detection. Currently, the most common position-detection scheme is back-focal-plane (BFP) interferometry (37, 38). Here, the interference between unscattered and forward-scattered light of a laser beam focused on a bead is used to provide positional information in the two lateral dimensions. By imaging the intensity distribution in the BFP of a condenser lens on a QPD or PSD, the recorded signals are rendered insensitive to the location of the trap in the field of view. A major advantage of these interference techniques is that the trapping laser can be used to perform trapping and position detection simultaneously. In this situation, the detection and trap are intrinsically aligned and only relative displacements of the bead with respect to the trap are measured. Displacements of typically up to a few hundred nanometers away from the center of the optical trap are directly proportional to the measured shift on the photodiodes in this configuration. On top of this, simultaneous video analysis of optical images can still be used to measure absolute positions and distances in the studied system.

Axial position detection – True three-dimensional position detection allows tracking the (suppressed) Brownian motion of the trapped particle and, thereby, fully quantifying the forces felt by the object in the optical trap. This can be accomplished by combining axial position detection with the abovementioned

lateral position-detection techniques. The axial position of trapped particles has been detected by using fluorescence methods, performing template-based analysis of bead images (as is often done in magnetic tweezers experiments, see Chapter 15), measuring the forward-scattered light intensity, or using nonimaging interference methods (6). The nonimaging axial interference method, in which modulations in the total laser intensity are detected in the BFP of the condenser, is most practical since it is accurate as well as easily combined with lateral interference-based detection. Contrary to lateral detection, the best axial sensitivity is obtained when only the low-NA fraction of the light is detected (39).

3.4. Trap Steering

If microscope stage movements do not provide enough flexibility to manipulate trapped objects, the trapping beam itself can be steered through the sample. This is particularly useful for steering multiple traps. Lateral trap movement can be achieved by changing the incoming angle of the trapping beam into the objective while axial movement is effected by changing the level of collimation of the beam.

In practice, such three-dimensional trap steering can be accomplished by moving the lenses in a telescope in front of the objective. Alternatively, the use of tip-tilt or galvanometric mirrors, for which accurate and reproducible positioning can be obtained through closed-loop feedback systems, allows rapid lateral trap movement up to several kHz. Finally, more advanced techniques for trap steering include acousto-optical deflectors (AODs) and electro-optical deflectors (EODs). These provide higher scanning speeds up to the MHz range, but typically have more limited deflection ranges. Additional drawbacks are the lower throughput efficiency and inhomogeneous diffraction of AODs and the high costs of EODs.

To avoid nonlinearities in the lateral trap steering, it is important to place the steering elements in the setup such that the angular deflection from the optical axis originates in planes conjugate to the BFP of the objective, such as the telescope configuration in Fig. 6. Otherwise, the transmitted laser power and, therefore, the trap stiffness will be dependent on the position in the sample. Finally, it is important to realize that trapped objects are limited in manipulation speed. Viscous drag causes the trapped particle to escape from the trap at high steering speeds.

If scanned across multiple positions, galvanometric mirrors and the even faster AODs or EODs can be used to generate multiple traps from a single laser source (see Fig. 7). If the laser is scanned rapidly enough, a trapped particle may not sense the transient absence of the optical trap when at the other scanned positions. This way of generating multiple traps is called trap multiplexing or “time sharing.” An alternative approach to generate multiple

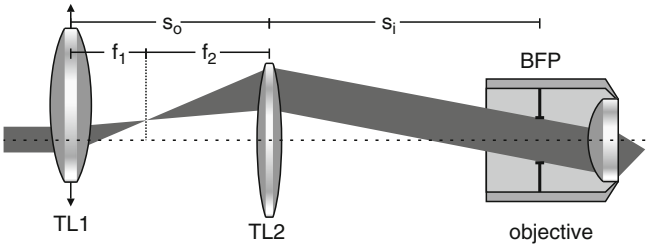

Fig. 6. Steering of an optical trap using a telescope configuration. The second telescope lens (TL2) images the plane of the first one (TL1) onto the back focal plane (BFP) of the objective: $1/s_i = 1/f_2 - 1/(f_1 + f_2)$. Lateral movement of the first telescope lens causes the incident collimated laser beam to enter the BFP under an angle. The laser focus in the sample, thereby, displaces laterally. No intensity changes occur when displacing the beam, hence keeping the trap stiffness position independent.

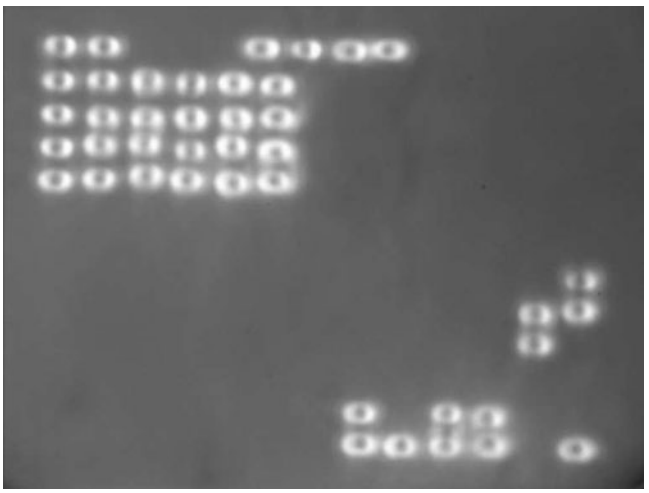

Fig. 7. Microscopy image of the time-shared optical trapping of 42 beads using AODs. This image demonstrates the smallest game of *Tetris* ever played. The corresponding video can be found online at http://www.nat.vu.nl/compl/dualdna/tetris.

traps from a single laser line is provided by diffractive optical elements, such as spatial light modulators (SLMs). Multiple trap generation and steering in this case rely on the holographic pattern that causes the incident laser to diffract into separate foci in the sample. The intricate computation of the holographic pattern practically limits the update rates with which the traps can be steered, although this technique is continuously improved. So far, holographic schemes based on SLMs have proven difficult to combine with position- and force-sensing schemes.

3.5. Environment of the Setup

To ensure stability and high spatial resolution, the environment of the optical tweezers setup needs to be well-controlled. Common

precautions include the use of passively damping optical tables and temperature stabilization within 0.5–0.1 K. Convection of the air in the optical pathway can induce beam deviations through local density fluctuations. These effects can be minimized by enclosing the optical path, reducing the optical path length, or reducing the number of foci along the optical path, since the beam is more sensitive to local density fluctuations in these focal points. For the most demanding applications, optical tweezers instruments have been placed in acoustically isolated rooms with air conditioning equipment that filters out dust particles in the air or even in enclosures in which ambient air is replaced by helium, the even lower refractive index of which renders the instruments less susceptible to density fluctuations of the gas (40).

3.6. Combining Optical Tweezers with Other Techniques

Optical tweezers instruments are composed of common microscopy components and are often incorporated into commercial microscopes. This makes it attractive to combine optical tweezers, and their high level of control, with the capabilities of other optical techniques in order to study biological systems in greater detail. The design of an optical tweezers instrument, however, directly influences its capabilities and to what extent other microscopy or related techniques can be integrated with it.

The counterpropagating beams layout, for instance, requires critical coaxial alignment, is difficult to implement in conventional microscopes, and puts strong restrictions on the optics and additional functionalities of the experimental setup. A single-beam optical trap, on the other hand, requires a tightly focused laser beam for stable trapping, which in turn requires a high-NA objective lens and a suitably expanded laser beam at the input aperture. Other than that, no strong requirements are imposed on the microscope, which renders the single-beam trap the more widely used configuration.

A new development is the integration of sensitive fluorescence microscopy with optical tweezers, as recently reviewed (30). The direct visualization of single molecules in controlled optical tweezers manipulation experiments has proven a powerful method for the detailed investigation of biomolecular systems, in particular for unraveling DNA–protein interactions (30, 41, 42). In these experiments, DNA is manipulated with optical tweezers while the binding and activity of proteins that interact with the DNA are directly observed through fluorescence microscopy. Changes in DNA structure due to DNA–protein interactions or movement of proteins along DNA can, thus, be simultaneously studied with force spectroscopy and fluorescence microscopy, providing a high level of versatility and unambiguity in these experiments. Furthermore, other advanced optical microscopy techniques, such as polarization or Raman spectroscopy, have been fruitfully combined with optical tweezers (43–46).

3.7. Optical Trapping Assays Employed in Biology

Several experimental layouts have been developed to employ optical tweezers in biology. The simplest layout consists of a single optical trap, in which particles can be manipulated and, optionally, forces between the trapped particle and its surroundings can be measured. A single optical trap has, for instance, been used to perform force spectroscopy on biomolecular systems that are tethered between the trap and a fixed substrate (see Fig. 2, top). Examples of experiments using this geometry include measurements of the mechanical and structural properties of biopolymers tethered between a trapped bead and a fixed substrate (i.e., a glass slide or a bead held by a micropipette (15)) and measurements of the forces involved in biomolecular activity (10, 20). This activity can be observed either directly, such as in the motion of motor proteins tethered to a trapped bead, or indirectly by measuring structural changes in biomolecules, such as DNA, due to enzymatic activity.

The fixed substrate can also be replaced by a particle trapped in a second optical trap (see Fig. 2, bottom). In this dual-trap assay, a biomolecular system tethered between two trapped beads can, thus, be fully suspended in solution, which prevents unwanted surface interactions. In addition, this layout suppresses noise associated with fluctuations or drift in the relative positions of the optical trap and a fixed substrate. This geometry has been employed to obtain single base pair resolution of RNA polymerase activity (40).

Finally, advanced optical trapping geometries include the use of multiple optical traps (see Fig. 7), which allow manipulating large biological structures and multiple colloidal particles (47–50). On the single-molecule level, multiple optical traps have been used to measure interactions of multiple DNA molecules and bound proteins (22, 51).

4. Commercial Optical Tweezers Systems

The design and construction of an optical tweezers instrument can be a tedious task, requiring practical and theoretical experience in fields ranging from laser physics, optics, thermodynamics, hydrodynamics, and analog and digital electronics to computer science in order to allow some level of computer control of the instrument as well as data acquisition. In addition, the maintenance of a home-built instrument can be time consuming as well. In view of that, it needs little explanation that many life science researchers hesitate to switch to this type of experimentation.

During the past decade, several companies have started offering commercial solutions for optical trapping experiments (23).

These solutions range from do-it-yourself kits, like that from Thorlabs or the miniTweezers from the Bustamante lab (see http://tweezerslab.unipr.it), to fully automated turnkey platforms. Recently, a product review appeared that describes and compares most commercial platforms (52). The review and the comparison chart therein make clear that optical tweezers technology has ripened over the past decades. Most manufacturers provide instruments that can be flexibly attached or integrated into a standard research-grade inverted optical microscope. Depending on the details of the instrument, this may leave open the possibility to configure the optical microscope in order to combine optical tweezers with other microscope techniques, as described above. However, when the optical trapping laser is coupled into the microscope through the fluorescence port, it is obviously difficult or impossible to combine optical tweezers and fluorescence microscopy.

A number of commercial suppliers offer optical tweezers instrumentation primarily as a micromanipulation add-on, integrated with microdissection equipment for controllably cutting cells or tissues. Both the Zeiss PALM product series and those from Molecular Machines and Industries (MMI) originate from the microdissection field. Others are designed as automated, precise force-sensing optical tweezers microscopes, such as the NanoTracker from JPK Instruments (see Figs. 5 and 8), which include sample-handling modules for microfluidics or live-cell work. The BioRyx 200 from Arryx Inc. focuses on the simultaneous manipulation of large groups of particles through holographic trap arrays.

Fig. 8. Dr. Remus T. Dame (Leiden University, The Netherlands) using his NanoTracker from JPK Instruments.

When considering the purchase of a commercial optical tweezers instrument, the aforementioned review may be a good starting point. Several aspects should be kept in mind. Obviously, the first thing to define is the main application for the instrument. Is the system going to be used only for manipulation, or is quantification of the forces exerted going to be useful? Is fluorescence imaging required, or are other microscope features important? Is the delivered software flexible enough to accommodate the required experiments? Important characteristics, like user friendliness or flexibility in system design, are best assessed in a live demonstration of the instrument.

5. Concluding Remarks

Optical tweezers techniques form a valuable addition to the single-molecule toolkit. These minimally invasive techniques provide scientists with the ability to actively manipulate biomolecules with nanometer precision and to measure or apply forces with piconewton resolution. Examples of the application of these powerful tools in molecular biology include the study of active molecular motors, the mechanical properties of DNA, and the mechanochemistry of DNA–protein interactions. Commercial optical tweezers systems are becoming increasingly available, which makes this powerful and versatile technique accessible to a broad range of researchers from different backgrounds and undoubtedly drives new biological discoveries on the single-molecule level. The following chapters describe detailed methods and protocols of several applications of optical tweezers in molecular biology.

References

1. Ashkin, A. (1970) Acceleration and Trapping of Particles by Radiation Pressure *Physical Review Letters* **24**, 156–9.
2. Ashkin, A., Dziedzic, J. M., Bjorkholm, J. E., and Chu, S. (1986) Observation of a single-beam gradient force optical trap for dielectric particles *Optics Letters* **11**, 288–90.
3. Chu, S. (1991) Laser manipulation of atoms and particles *Science* **253**, 861–6.
4. Chu, S. (1992) Laser trapping of neutral particles *Scientific American* **266**, 70–6.
5. Svoboda, K., and Block, S. M. (1994) Biological Applications of Optical Forces *Annual Review of Biophysics & Biomolecular Structure* **23**, 247–85.
6. Neuman, K. C., and Block, S. M. (2004) Optical trapping *Review of Scientific Instruments* **75**, 2787–809.
7. Moffitt, J. R., Chemla, Y. R., Smith, S. B., and Bustamante, C. (2008) Recent Advances in Optical Tweezers *Annual Review of Biochemistry* **77**, 205–28.
8. Ashkin, A., and Dziedzic, J. M. (1987) Optical trapping and manipulation of viruses and bacteria *Science* **235**, 1517–20.
9. Ashkin, A., Dziedzic, J. M., and Yamane, T. (1987) Optical trapping and manipulation of single cells using infrared-laser beams *Nature* **330**, 769–71.
10. Block, S. M., Goldstein, L. S. B., and Schnapp, B. J. (1990) Bead Movement by Single

Kinesin Molecules Studied with Optical Tweezers *Nature* **348**, 348–52.

11. Bustamante, C., Macosko, J. C., and Wuite, G. J. L. (2000) Grabbing the cat by the tail: Manipulating molecules one by one *Nature Reviews Molecular Cell Biology* **1**, 130–6.
12. Davenport, R. J., Wuite, G. J. L., Landick, R., and Bustamante, C. (2000) Single-molecule study of transcriptional pausing and arrest by E. coli RNA polymerase *Science* **287**, 2497–500.
13. Smith, S. B., Cui, Y., and Bustamante, C. (1996) Overstretching B-DNA: the elastic response of individual double-stranded and single-stranded DNA molecules *Science* **271**, 795–9.
14. Svoboda, K., Schmidt, C. F., Schnapp, B. J., and Block, S. M. (1993) Direct Observation of Kinesin Stepping by Optical Trapping Interferometry *Nature* **365**, 721–7.
15. Wuite, G. J. L., Smith, S. B., Young, M., Keller, D., and Bustamante, C. (2000) Single-molecule studies of the effect of template tension on T7 DNA polymerase activity *Nature* **404**, 103–6.
16. EssevazRoulet, B., Bockelmann, U., and Heslot, F. (1997) Mechanical separation of the complementary strands of DNA *Proceedings of the National Academy of Sciences of the United States of America* **94**, 11935–40.
17. Kellermayer, M. S. Z., and Bustamante, C. (1997) Folding-unfolding transitions in single titin molecules characterized with laser tweezers (vol 276, pg 1112, 1997) *Science* **276**, 1112–6.
18. Tskhovrebova, L., Trinick, J., Sleep, J. A., and Simmons, R. M. (1997) Elasticity and unfolding of single molecules of the giant muscle protein titin *Nature* **387**, 308–12.
19. Wang, M. D., Schnitzer, M. J., Yin, H., Landick, R., Gelles, J., and Block, S. M. (1998) Force and velocity measured for single molecules of RNA polymerase *Science* **282**, 902–7.
20. Yin, H., Wang, M. D., Svoboda, K., Landick, R., Block, S. M., and Gelles, J. (1995) Transcription against an applied force *Science* **270**, 1653–7.
21. Bustamante, C., Bryant, Z., and Smith, S. B. (2003) Ten years of tension: single-molecule DNA mechanics *Nature* **421**, 423–7.
22. Dame, R. T., Noom, M. C., and Wuite, G. J. L. (2006) Bacterial chromatin organization by H-NS protein unravelled using dual DNA manipulation *Nature* **444**, 387–90.
23. Matthews, J. N. A. (2009) Commercial optical traps emerge from biophysics labs *Physics Today* **62**, 26–8.
24. Ashkin, A. (1992) Forces of a Single-Beam Gradient Laser Trap on a Dielectric Sphere in the Ray Optics Regime *Biophysical Journal* **61**, 569–82.
25. Gittes, F., and Schmidt, C. F. (1998) Signals and noise in micromechanical measurements, in *Methods in Cell Biology*, pp 129–56, Academic Press, London.
26. Reif, F. (1965) *Fundamentals of statistical and thermal physics*, McGraw Hill, New York.
27. Peterman, E. J. G., Gittes, F., and Schmidt, C. F. (2003) Laser-induced heating in optical traps *Biophysical Journal* **84**, 1308–16.
28. Vermeulen, K. C., Wuite, G. J. L., Stienen, G. J. M., and Schmidt, C. F. (2006) Optical trap stiffness in the presence and absence of spherical aberrations *Applied Optics* **45**, 1812–9.
29. Guck, J., Ananthakrishnan, R., Mahmood, H., Moon, T. J., Cunningham, C. C., and Kas, J. (2001) The optical stretcher: A novel laser tool to micromanipulate cells *Biophysical Journal* **81**, 767–84.
30. van Mameren, J., Peterman, E. J. G., and Wuite, G. J. L. (2008) See me, feel me: methods to concurrently visualize and manipulate single DNA molecules and associated proteins *Nucleic Acids Research* **36**, 4381–9.
31. Brewer, L. R., and Bianco, P. R. (2008) Laminar flow cells for single-molecule studies of DNA-protein interactions *Nature Methods* **5**, 517–25.
32. Mahamdeh, M., and Schaffer, E. (2009) Optical tweezers with millikelvin precision of temperature-controlled objectives and base-pair resolution *Optics Express* **17**, 17190–9.
33. Cheezum, M. K., Walker, W. F., and Guilford, W. H. (2001) Quantitative comparison of algorithms for tracking single fluorescent particles *Biophysical Journal* **81**, 2378–88.
34. Crocker, J. C., and Grier, D. G. (1996) Methods of digital video microscopy for colloidal studies *Journal of Colloid and Interface Science* **179**, 298–310.
35. Finer, J. T., Simmons, R. M., and Spudich, J. A. (1994) Single myosin molecule mechanics - piconewton forces and nanometer steps *Nature* **368**, 113–9.
36. Visscher, K., Gross, S. P., and Block, S. M. (1996) Construction of multiple-beam optical traps with nanometer-resolution position sensing. *IEEE Journal of Selected Topics in Quantum Electronics* **2**, 1066–76.
37. Denk, W., and Webb, W. W. (1990) Optical measurement of picometer displacements of transparent microscopic objects *Applied Optics* **29**, 2382–91.

38. Gittes, F., and Schmidt, C. F. (1998) Interference model for back-focal-plane displacement detection in optical tweezers *Optics Letters* **23**, 7–9.
39. Dreyer, J. K., Berg-Sorensen, K., and Oddershede, L. (2004) Improved axial position detection in optical tweezers measurements *Applied Optics* **43**, 1991–5.
40. Abbondanzieri, E. A., Greenleaf, W. J., Shaevitz, J. W., Landick, R., and Block, S. M. (2005) Direct observation of base-pair stepping by RNA polymerase *Nature* **438**, 460–5.
41. van Mameren, J., Gross, P., Farge, G., Hooijman, P., Modesti, M., Falkenberg, M., Wuite, G. J. L., and Peterman, E. J. G. (2009) Unraveling the structure of DNA during overstretching by using multicolor, single-molecule fluorescence imaging *Proceedings of the National Academy of Sciences of the United States of America* **106**, 18231–6.
42. van Mameren, J., Modesti, M., Kanaar, R., Wyman, C., Peterman, E. J. G., and Wuite, G. J. L. (2009) Counting RAD51 proteins disassembling from nucleoprotein filaments under tension *Nature* **457**, 745–8.
43. Bennink, M. L., Scharer, O. D., Kanaar, R., Sakata-Sogawa, K., Schins, J. M., Kanger, J. S., de Grooth, B. G., and Greve, J. (1999) Single-molecule manipulation of double-stranded DNA using optical tweezers: interaction studies of DNA with RecA and YOYO-1 *Cytometry* **36**, 200–8.
44. Murade, C. U., Subramaniam, V., Otto, C., and Bennink, M. L. (2010) Force spectroscopy and fluorescence microscopy of dsDNA-YOYO-1 complexes: implications for the structure of dsDNA in the overstretching region *Nucl. Acids Res.*
45. Petrov, D. V. (2007) Raman spectroscopy of optically trapped particles *Journal of Optics A: Pure and Applied Optics* **9**, S139-S56.
46. Rao, S., Bálint, t., Cossins, B., Guallar, V., and Petrov, D. (2009) Raman Study of Mechanically Induced Oxygenation State Transition of Red Blood Cells Using Optical Tweezers **96**, 209–16.
47. Grier, D. G. (2003) A revolution in optical manipulation *Nature* **424**, 810–6.
48. Liesener, J., Reicherter, M., Haist, T., and Tiziani, H. J. (2000) Multi-functional optical tweezers using computer-generated holograms *Optics Communications* **185**, 77–82.
49. Mio, C., Gong, T., Terray, A., and Marr, D. W. M. (2000) Design of a scanning laser optical trap for multiparticle manipulation *Review of Scientific Instruments* **71**, 2196–200.
50. Visscher, K., Brakenhoff, G. J., and Krol, J. J. (1993) Micromanipulation by multiple optical traps created by a single fast scanning trap integrated with the bilateral confocal scanning laser microscope *Cytometry* **14**, 105–14.
51. Noom, M. C., van den Broek, B., van Mameren, J., and Wuite, G. J. L. (2007) Visualizing single DNA-bound proteins using DNA as a scanning probe *Nature Methods* **4**, 1031–6.
52. Piggee, C. (2008) Optical tweezers: not just for physicists anymore *Analytical Chemistry* **81**, 16–9.